The Cryosphere Discuss., 9, 1047–1075, 2015
www.the-cryosphere-discuss.net/9/1047/2015/
doi:10.5194/tcd-9-1047-2015

The Cryosphere Discussions
Open Access

Microscale variability of snow depth using U.A.S. technology

C. De Michele[1], F. Avanzi[1], D. Passoni[1], R. Barzaghi[1], L. Pinto[1], P. Dosso[2], A. Ghezzi[1], R. Gianatti[3], and G. Della Vedova[3]

[1]Politecnico di Milano, Department of Civil and Environmental Engineering,
Piazza Leonardo da Vinci 32, 20133 Milano, Italy
[2]Studio di Ingegneria Terradat, Paderno Dugnano, Italy
[3]a2a Group, Grosio, Italy

Received: 21 January 2015 – Accepted: 1 February 2015 – Published: 20 February 2015

Correspondence to: C. De Michele (carlo.demichele@polimi.it)

Published by Copernicus Publications on behalf of the European Geosciences Union.

Abstract

We investigate the capabilities of photogrammetry-based surveys with Unmanned Aerial Systems (U.A.S.) to retrieve the snow depth distribution at cm resolution over a small alpine area (∼ 300 000 m^2). For this purpose, we have designed two field campaigns during the 2013/2014 winter season. In the first survey, realized at the beginning of the accumulation season, the digital elevation model of bare soil has been obtained. The second survey, made at the end of the accumulation season, allowed to determine the snow depth distribution as difference with respect to the previous aerial survey. 12 manual measurements of snow depth were collected at random positions in order to run a point comparison with U.A.S. measurements. The spatial integration of U.A.S. snow depth measurements allowed to estimate the snow volume accumulated over the area. We compare this volume estimation with the ones provided by classical interpolation techniques of the 12 point measurements. Results show that the U.A.S. technique provides an accurate estimation of point snow depth values (the average difference with reference to manual measurements is of −7.3 cm), and a distributed evaluation of the snow accumulation patterns. Moreover, the interpolation techniques considered return average differences in snow volume estimation, with respect to the one obtained through the U.A.S. technology, equal to ∼ 21 %.

1 Introduction

Seasonal snow accumulation and ablation dynamics are highly variable in space and time (Elder et al., 1991; Grünewald et al., 2010, 2013; Mott et al., 2011; Scipión et al., 2013; Winstral et al., 2013). This variability plays a key role, among others, in avalanche prediction (Schweizer et al., 2008), in the routing of melt water in snowpacks (Katsushima et al., 2013; Hirashima et al., 2014), in melt-runoff modeling (Lundquist and Dettinger, 2005), and in the evaluation of snow water equivalent distribution on complex terrains (Bavera et al., 2014).

The principal forcings ruling the spatial heterogeneity in the seasonal snowpack include (1) orographic effects (Lehning et al., 2008; Mott et al., 2014), (2) elevation (Avanzi et al., 2014a), mainly ruling rain-snow transition zone, i.e. the elevation which separates snow- and rain-dominated areas during winter (Marks et al., 2013; Hinckley et al., 2014; Klos et al., 2014), (3) aspect and shadows from surrounding terrain (Hock, 1999; Marsh et al., 2012), which influence the exposure to short- and long-wave radiation input from the Sun, hence varying melting rates, (4) wind redistribution (Lehning et al., 2008; Mott and Lehning, 2010), (5) avalanche transport (Lehning and Fierz, 2008; Grünewald et al., 2013) and (6) vegetation (Golding and Swanson, 1986; Ellis et al., 2010; Pomeroy et al., 2012).

The spatial distribution of snow depth and snowpack mass content, in the form of Snow Water Equivalent, SWE, has been widely measured and modeled, both at the local, slope and catchment scale (Grünewald et al., 2010). Modeling approaches include statistical attempts, such as Carroll and Cressie (1996), Elder et al. (1998), Erxleben et al. (2002), Anderton et al. (2004), Molotch et al. (2004), Dressler et al. (2006), López Moreno and Nogués-Bravo (2006), Skaugen (2007) and Bavera et al. (2014), and physically-based models, e.g. Lehning et al. (2006, 2008). These works have improved our knowledge about, e.g. the relevance of single forcings in determining the distribution of the snow cover on complex terrains (Anderton et al., 2004). In addition, they provide a useful tool to estimate the impact of future modifications of climate on the Earth system (Bavay et al., 2009, 2013). Nonetheless, many input data are usually needed, together with great computational efforts (Bavera et al., 2014).

On the experimental side, automatic snowpack mass dynamics monitoring has been traditionally run by means of point devices, such as snow pillows (Cox et al., 1978), cosmic ray counters (Morin et al., 2012) and ultrasonic depth sensors (Ryan et al., 2008). These sensors are usually placed in areas that are believed to be suitable locations for representative measurements at wider scales (i.e. unaffected by local heterogeneities). Nonetheless, Grünewald and Lehning (2014) demonstrate that, usually, point stations on flat areas tend to overestimate catchment mean snow depth, and that representa-

TCD
9, 1047–1075, 2015

tive cells are usually randomly located, i.e. impossible to be determined a priori. These represent important drawbacks of point weather stations in the study of snowpack dynamics (see again Grünewald and Lehning (2014) and references therein). Moreover, these are usually affected by systematic and random errors (Cox et al., 1978; Fassnacht, 2004; Johnson, 2004), that decrease the actual precision of measurements with respect to instrumental resolution (Avanzi et al., 2014b).

On the other hand, increasing interest is nowadays growing around distributed measurements of snow extent, depth and SWE (Dietz et al., 2012), able to substitute, or integrate, point, and usually sparse, measurements of these quantities. Tested techniques include LIDAR (Light Detection and Ranging, see e.g. Hopkinson et al., 2004, 2012; Deems et al., 2006, 2013; Dadic et al., 2010; Hedrick et al., 2014), terrestrial or airborne laser scanning (Prokop et al., 2008; Grünewald et al., 2010; Lehning et al., 2011; Grünewald et al., 2013; Grünewald and Lehning, 2014), SAR (Synthetic Aperture Radar, Luzi et al., 2009), aerial photographies (Blöschl and Kirnbauer, 1992; König and Sturm, 1998; Worby et al., 2008), time-lapse photography (Farinotti et al., 2010), optical and micro-waves data from satellite platforms, such as MODIS, AVHRR or ENVISAT (Parajka and Blöschl, 2006; Dietz et al., 2012). In this perspective, a future target could be the realization of automatic and repeatable surveys at a fine spatial resolution (say, a centimeter resolution both in the horizontal and vertical direction).

Here, we have investigated the possibility of using Unmanned Aerial Systems (U.A.S., sometimes also referred to as drones) to measure snow depth patterns within a small mountainous basin at cm resolution. U.A.S. represent an alternative to aforementioned techniques to automatically, cheaply (Colomina and Molina, 2014) and autonomously reconstruct a high-resolution Digital Surface Model (hereinafter, DSM) of a given area (Watts et al., 2012). Thus, they potentially allow to obtain an automatic and detailed description of snow depth variability. We chose as a field test the bare plateau around the Malghera lake, within the western Val Grosina valley (around 2300 m a.s.l.), northern Italy. A double airborne survey of this area, at the beginning and end of the accumulation season, was designed. During the first one, on 26 September 2013, the

DSM of the bare soil has been collected, while during the second one, on 11 April 2014, the same area has been surveyed to determine the DSM of the snow cover. Then, calculating the vertical differences between the two DSMs (Deems et al., 2013), the spatial distribution of snow depth has been derived, and compared with manual measurements at 12 points. These locations have been randomly chosen. Successively, the snow volume accumulated over the area was determined. This has been compared to the ones provided by classical interpolation techniques (namely arithmetic mean, inverse distance weighting, Thiessen method and kriging) of point measurements.

In Sect. 2, we describe the study area, while in Sect. 3, we provide some information about the U.A.S. technology, the design of the two surveys, the comparison with point measurements, and the spatialization techniques used as a matter of comparison. Section 4 gives results and discussion, while in Sect. 5 conclusions are given, and some outlooks are illustrated.

2 The study area

The case study is located in the western Val Grosina valley, Lombardy region, northern Italy. It is nearby the Malghera lake, $\sim 46°20'2''$ N, $\sim 10°7'14''$ E, 2320 m a.s.l. The approximate extent of the study area is 300 000 m^2. In Fig. 1, the location of the study area is given, together with the topographic map of the bare soil, produced by the local regional administration. Figure 1 shows that site topography is relatively homogeneous.

The study area has been selected according to the following criteria: (1) it must have a quite high elevation (> 2000 m a.s.l.), to guarantee an adequate snow thickness at the end of the accumulation season; (2) it must be easily accessible during all the seasons; (3) it must be interested by seasonal snow, so that the DSM acquired during autumn represents the 3-D surface of the soil.

TCD
9, 1047–1075, 2015

Title Page
Abstract Introduction
Conclusions References
Tables Figures
◀| |▶
◀ ▶
Back Close
Full Screen / Esc
Printer-friendly Version
Interactive Discussion

3 Methods

3.1 U.A.S. technology and design of the surveys

The use of U.A.S. is nowadays rapidly increasing (Eisenbeiss, 2009; Watts et al., 2012; Colomina and Molina, 2014). Some examples include ecology (Dunford et al., 2009; Koh and Wich, 2012), coastal engineering (Delacourt et al., 2009) or geomorphological mapping (Lejot et al., 2007; Hugenholtz et al., 2013). See Colomina and Molina (2014) for an exhaustive review.

These systems provide an airborne support for sensors operating at different wavelengths. The support can autonomously determine its position in a 3-D reference system. Therefore, it is able to reproduce a pre-arranged flight plan. This let for autonomous, repeteable, cheap (Colomina and Molina, 2014) and low-risk surveys to be run, even in high-wind and hard climate conditions (Funaki et al., 2008). In optical surveys, usually they use compact digital cameras, due to the limited payload (say $\sim 10^2$ g). Nonetheless, these are affected by higher deformations as compared with those of photogrammetric calibrated cameras (Pollefeys et al., 1999; Remondino, 2006; Stretcha et al., 2010; Sona et al., 2014).

The U.A.S. used in the two surveys is a light-weight fixed wing SwingletCAM system (SenseFly®). It is characterized by a limited weight (< 500 g) and size (wingspan equal to 80 cm). These features make it suitable to perform photogrammetric flights over limited areas (about 1 km^2) at very high resolutions (3–7 cm of Ground Sample Distance – GSD). The SwingletCAM is able to perform pre-planned flights in a fully automated mode. The device continuously analyzes data from the onboard GPS/IMU and takes care of all aspects of the flight mission. However, the operator can always recover full control of the system itself. The system incorporates a compact camera Canon Ixus 220HS (12 Mp and fixed focal length of 4.0 mm) which can acquire images at a GSD of some cm (depending on flight height).

In the two field surveys, the GSD was set to 4.5 cm. Thus, we obtained an average flight height of 132 m a.g.l. (the range of the height values is between 130 and 135 m).

TCD
9, 1047–1075, 2015

Furthermore, in order to gain the maximum stereoscopy and to avoid uncovered areas, forward and side overlaps were set to 80 %. Following this approach, from six to seven strips were necessary to cover the area of interest.

3.2 Comparison with point measurements

In what follows, we compare estimates of snow depth obtained by the SwingletCAM at some points where point manual measurements are operated using snow poles. The locations of these measurements have been randomly chosen. Snow poles have been often used since the beginning of snow field surveys to determine snow depth amount at a point, in the context of snow density and SWE determination (Church, 1933). Although they represent the most direct way to measure this quantity, the long time needed to operate these surveys (Deems et al., 2013) have caused their partial replacement with automatic devices. A comparison with probe measurements has been often used to assess the performances of alternative techniques to describe snow depth dynamics (Deems et al., 2013).

However, no specific rule or common practice exists in the literature to determine the minimum number of manual snow depth measurements, over a given area, needed to evaluate the performances of a given technique. As an example, Machguth et al. (2006) included 19 measurements of snow depth with snow probes and 20 snow pits in the assessment of helicopter-borne GPR performances over two glaciers in the Alps (area $\sim 17.3\,\mathrm{km}^2$), Prokop et al. (2008) used automatic measurements and 90 bamboo sticks to record snow depth changes and to compare with laser scanning and tachimetry estimations over a $\sim 200\,\mathrm{m} \times 200\,\mathrm{m}$ area, Bavera and De Michele (2009) considered 170 point snow depth measurements to validate snow distribution estimations at a basin scale (area $325\,\mathrm{km}^2$, snow cover interesting 2/3 of the total surface), while Gutmann et al. (2012) and Nievinski and Larson (2014) used manual measurements from either 4 or 1 snow poles respectively to evaluate GPS-based estimations of snow depth. In this framework, we operated 12 poles measurements over $\sim 300\,000\,\mathrm{m}^2$, i.e. approximately one measurement every $25\,000\,\mathrm{m}^2$. No automatic device was available in the

TCD
9, 1047–1075, 2015

study area. These point measurements allowed to make a statistical evaluation (i.e. calculating mean and SD) of the performances of U.A.S. in retrieving snow depth at a generic point within the study area.

3.3 Spatial interpolation techniques

Spatial interpolation techniques are methods used in the literature to produce continuous maps of attributes starting from some point values. These methods have been widely used in snow hydrology applications to produce maps of snow depth variability (López Moreno and Nogués-Bravo, 2006) starting from point values of the same variable.

These techniques include, among others, (1) the *Inverse Distance Weighting* mehod (IDW), that calculates the attribute at a given location as a function of the distance between that point and the locations where known values are given (Erxleben et al., 2002; Fassnacht et al., 2003; López Moreno and Nogués-Bravo, 2006; Bavera et al., 2014), (2) *Thiessen* method, that associates the data at a given location to a certain subset of points close to it (Elder et al., 1991), (3) *Kriging*, which estimates the unknown values by previously estimating (or assigning) a certain law of variation of the variable in space (the so-called variogram, Carroll and Cressie, 1996; Balk and Elder, 2000; Erxleben et al., 2002; López Moreno and Nogués-Bravo, 2006), (4) *Cokriging*, that adds to the variogram additional predictors, such as elevation or aspect (López Moreno and Nogués-Bravo, 2006), (5) *Cokriging of the residuals* (Erxleben et al., 2002) and (6) *Spline*, that estimates unknown values by using a function that minimizes surface curvature (López Moreno and Nogués-Bravo, 2006). Moreover, global methods such as regression-tree models, multivariate statistical analysis or linear models have been also applied (Erxleben et al., 2002; Fassnacht et al., 2003; Anderton et al., 2004; Dressler et al., 2006; López Moreno and Nogués-Bravo, 2006; Bavera et al., 2014), sometimes combined with remote sensed images (such as in Harshburger et al., 2010).

Here, we consider some classical spatial interpolation techniques, and we compare their estimates of snow volume with the one obtained using U.A.S. These techniques

TCD
9, 1047–1075, 2015

are inverse distance weighting, Thiessen method, and ordinary Kriging. In addition, we will consider also the arithmetic mean of snow depth measured at poles.

4 Results

4.1 Surveys realization

For both the two surveys, the flight lasted around 15–20 min. In the survey made on 26 September 2013, the U.A.S. collected a block of 47 images divided in 6 strips. Due to the high image overlap, all the ground points are visible in many images (from 3 to 9, see the left panel of Fig. 2). Thirteen pre-signalized Ground Control Points (henceforth, GCPs), measured through GPS rapid static survey, allowed the referencing of the block and the accuracy analyses. The SD of the three coordinates of GCPs are around 3 cm in the horizontal components, and 5 cm in the vertical one.

In the survey run on 10 April 2014, the U.A.S. collected a block of 84 images divided in 12 strips (6 regular strips as in the autumn survey plus 6 cross strips). Fourteen pre-signalized GCPs, measured through a GPS static survey and theodolite, allowed the referencing of the block. This set of GCPs is different from the one used during the first survey. We chose points that were reasonably distributed over the area, and we referred them to the same reference frame. Based on this survey, GCPs coordinates have been estimated with a SD of about 1 cm.

The blocks of images were processed using the Agisoft Photoscan software. It is a 3-D modelling software, carrying out the image relative orientation, together with the self-calibration, in an arbitrary reference system, which is often obtained using a minimum constraint coming from the approximate orientation provided by the telemetry. Firstly, for each block of images, the position of the camera for each image is determined searching common points on the images. Then the extraction of topographic points (which represent a cloud of points), and the rejection of outliers are made for

TCD
9, 1047–1075, 2015
Snow depth variability using U.A.S.
C. De Michele et al.

each survey. The subsequent use of GCPs allows translating and rotating the photogrammetric blocks in a specific reference frame, i.e. ETRF2000.

We report in Fig. 2 the location of camera photos and their overlap for each of the two surveys. In particular, the left panel regards the survey made on September 2013, while the right panel refers to the survey run during April 2014. Colors indicate the number of images covering each area. It is well known that the precision in coordinates estimation increases with an increasing number of images in which a point is present (Remondino and El-Hakim, 2006). In this perspective, most of the study area has been imaged at least by 3 or 4 images. Clearly, the overlap increases at the center of the study area. In that area, points have been imaged by a number of images ≥ 9.

4.2 DSMs production

Using the Agisoft Photoscan software, we have obtained orhophotos and DSMs of the two surveys from the clouds of points as 3-D polygonal meshes.

Figure 3a and c, shows the orthophoto for the autumn and the spring survey, respectively. Figure 3b and d, describes the related DSMs, both characterized by a pixel size of 5 cm. Red lines depict contour lines (10 m interval).

The autumn ortophoto (Fig. 3a) shows high coherence with the topographic map in scale 1 : 10 000, produced by the regional administration, and reported as background. For example, rivers and Malghera Lake outlet are correctly located. This consideration holds from the quantitative point of view, because contour lines of the topographic map (in black) and those of DSM (in red) are in agreement (see Fig. 3b).

As for the spring survey (Fig. 3c and d), a comparison with the topographic map is not straightforward, because of snow depth coverage. Nevertheless, rivers and lake outlet seems to have been correcty positioned, since they correspond to clear depressions in snow coverage. The snow depth surface on this area is interested by patchy coverage of sand dust transported by wind storms. This is visible as brown areas in the ortophoto (Fig. 3c), and has been of great help in referencing the images of the spring survey, providing common points on photographs. Clearly, the associated DSM shows contour lines which are different from the ones obtained during the September survey. This is an effect of snow depth presence on the ground. This causes a slight reduction in topography irregularities, too.

4.3 Point snow depth retrieval

We report in Table 1 a comparison between manual (H_M) and U.A.S. based ($H_{U.A.S.}$) snow depth measurements. Manual measurements are associated with a standard resolution of ±1 cm. The average difference between measurements is equal to −7.3 cm, with an associated SD of 12.8 cm. This result shows that the U.A.S. technique is able to locally estimate the snow depth values with a precision of ∼ 10 cm. Part of this difference could be explained by slight differences in the position of manual measurements and U.A.S. estimates. Nonetheless, this precision is comparable with the order of magnitude of the precision (instrumental resolution and noise effect) of many automatic sensors currently installed for point measurements of the same variable (Avanzi et al., 2014b).

4.4 Distributed estimation of snow depth

Figure 4 reports a map of snow depth distribution over the study area, obtained making the difference of the elevations of the maps reported in Fig. 3. Different colors indicate different values of snow thickness (see the legend scale reported in the figure). Black dots indicate the location of the 12 manual measurements (already used in Sect. 4.3).

Snow depth shows a remarkable micro-topographic variability over the considered area, although this is rather limited in extension (around 300 000 m^2), and characterized by bare soil and scarce vegetation. Most of the central area is characterized by an alternation of low and high values of snow thicnkess, that would be completely missed by sampling at poles positions, only. Clusters of high values of snow depth correspond to the location of rivers, or depressions in micro-topography. On the contrary, low snow depths are observed on topographic local maxima.

Legend scale shows that micro-topographic differences can be equal to ∼ 2–3 m. This illustrates the importance of sampling resolution, the extreme variation of accumulation dynamics of snow depth, and the scarce representativeness of point measurements (Grünewald and Lehning, 2014).

The snow depth value at poles positions varies between 1.48 and 2.11 m. This represents a reduced variability with respect to the complete range of variation of U.A.S. snow depth values. On the one hand, the location of poles was randomly chosen, and snow depth spatial patterns are hardly predictable a priori (Grünewald and Lehning, 2014). On the other hand, additional investigations are necessary to assess U.A.S. performances in case of, e.g. shallow or patchy snow cover conditions.

Table 2 proposes a comparison of average/maximum/minimum snow depth and the estimated volume of snow depth using different spatial resolutions of the DSMs: 5, 10, 20 cm. Clearly, an increase of the spatial resolution would increase the number of pixels. Nevertheless, this would marginally affect the values of average/maximum/minimum snow depth, as also the estimated volume of snow. We can suggest a spatial resolution of 20 cm as a good trade off between the number of pixels considered and the description of the snow micro-topography. However, as a matter of continuity throughout the manuscript, we will use the DSM with a spatial resolution of 5 cm in the comparison with the classical interpolation techniques.

4.5 The comparison with classical interpolation techniques

Table 3 reports the comparison between the estimated snow volume using a set of simple interpolation techniques of the 12 snow depth poles (namely, arithmetic mean, IDW, Thiessen method and ordinary Kriging) and the estimation of snow volume operated by the U.A.S. system. The snow volume plays a key role in estimating the total amount of water in the snow form.

Results show that the differences among the estimates of different interpolation techniques are rather reduced. These are ∼ 1000 m^3, with the total volume equal to ∼ 360 000 m^3. Nonetheless, all these techniques greatly underestimate the snow volume estimated by the U.A.S. system (∼ 460 000 m^3). The average percentage difference in snow volume estimation, with respect to the one estimated by the U.A.S. system, is equal to ∼ 21 %. In terms of absolute values, the average difference is ∼ 96 350 m^3. Considering an average bulk snow density of 450 kg m^{-3} (measured at the same location during the April survey by means of a snow pit), this would entail an absolute difference in SWE estimation of ∼ 43 358 m^3.

It is worth recalling that the considered area has a very reduced extension with respect to the usual distance between gauged sites in instrumental networks (see e.g. Fassnacht et al., 2003). This result shows that the assessment of snow depth micro-topography has clear impacts on many applications of scientific as well as engineering interest (such as water availaibility estimation for civil usage and/or energy production), and cannot be easily neglected. From this perspective, U.A.S. systems confirm to be able to easily, cheapily, and semi-automatically return a more refined representation of snow depth.

Table 3 shows that all interpolation techniques return an underestimated volume of snow. This should be considered as a case-specific result, that is due to the choice of pole positions. In fact, Fig. 4 shows that manual measurements were taken in areas that were not characterized by very high snow cover. Since evaluating a-priori representative locations is very difficult (Grünewald and Lehning, 2014), and since they could even vary from year to year basing on snow redistribution dynamics, this result shows again the advantage of using a directly distributed estimation instead of relying on a simplified representation of snow topography.

5 Conclusions

For the first time, we have here assessed the possibility of retrieving snow depth microscale variability by means of a photogrammetry-based survey using a U.A.S. technology, over a small alpine area (∼ 300 000 m^2). For this purpose, we run two surveys. The first one, during September 2013, allowed to reconstruct the topography of the bare soil. This survey will not be necessary for future assessment of snow distribution in the same area. Then, during April 2014, a second survey allowed to reconstruct the microscale variability of snow depth, by vertical differentiation of the maps.

Results show that: (1) ortophoto and DSM of autumn survey are in agreement with the topographic map available for the study area; (2) the average difference between manual and U.A.S. based measurements of snow depth is competitive with typical precisions of point measurements (average difference equal to −7.3 cm, with an associated SD of 12.8 cm); (3) the evaluation of snow depth volume (hence, SWE) using classical interpolation techniques of point values of snow depth is severely biased (average difference in snow volume estimation, with respect to the one estimated by the U.A.S., equal to ∼ 21 %).

The U.A.S. technology has some interesting potentialities within the framework of available methods to reconstruct the spatial variability of snow surface. In fact, this device allows to obtain semi-automatic, quick and repeteable surveys of limited areas (∼ 300 000 m^2), with a very high vertical precision (SD ± 0.128 m in the vertical direction). Although the device that we used here needs the operator to assist it during take-off operations, other devices (currently not available to the authors) can take off and land in an autonomous way, and can cover much wider areas. This could let repeated (say, daily) surveys to be autonomously obtained, even without needing a operator to reach (or point from the distance) the target area. This, together with the possibility to substitute, or integrate, optical sensors with sensors at different wavelenghts, could represent in the future an alternative to automatic point stations to directly obtain distributed measurements of snow variables. Moreover, attempts have been already made to design supports that are able to resist to harder climatic conditions (Funaki et al., 2008), such as strong winds, that would make unfeasible a survey using the same sensor used here.

Future developments should compare the performances of this technique with the ones obtained by other remote sensing approaches, in similar conditions. Moreover, performances should be assessed during different weather conditions (such as during

TCD
9, 1047–1075, 2015
Snow depth variability using U.A.S.
C. De Michele et al.

precipitation events, or in conditions of scarce visibility), during different snow cover conditions (such as shallow snow covers), and/or in different topographic areas.

Acknowledgements. The Authors want to thank A2A for the logistic support during the set up of the experiment. We would like to thank Riccardo Capetti and Amilcare Marchetti (A2A) for their assistance during field activities.

References

Anderton, S. P., White, S. M., and Alvera, B.: Evaluation of spatial variability in snow water equivalent for a high mountain catchment, Hydrol. Process., 18, 435–453, doi:10.1002/hyp.1319, 2004. 1049, 1054

Avanzi, F., De Michele, C., and Ghezzi, A.: Liquid-solid partitioning of precipitation along an altitude gradient and its statistical properties: an Italian case study, Am. J. Clim. Change, 3, 71–82, doi:10.4236/ajcc.2014.31007, 2014a. 1049

Avanzi, F., De Michele, C., Ghezzi, A., Jommi, C., and Pepe, M.: A processing modeling routine to use SNOTEL hourly data in snowpack dynamic models, Adv. Water Resour., 73, 16–29, 2014b. 1050, 1057

Balk, B. and Elder, K.: Combining binary decision tree and geostatistical methods to estimate snow distribution in a mountain watershed, Water Resour. Res., 36, 13–26, doi:10.1029/1999WR900251, 2000. 1054

Bavay, M., Lehning, M., Jonas, T., and Löwe, H.: Simulations of future snow cover and discharge in Alpine headwater catchments, Hydrol. Process., 23, 95–108, doi:10.1002/hyp.7195, 2009. 1049

Bavay, M., Grünewald, T., and Lehning, M.: Response of snow cover and runoff to climate change in high Alpine catchments of Eastern Switzerland, Adv. Water Resour., 55, 4–16, doi:10.1016/j.advwatres.2012.12.009, 2013. 1049

Bavera, D. and De Michele, C.: Snow water equivalent estimation in the Mallero basin using snow gauge data and MODIS images and fieldwork validation, Hydrol. Process., 23, 1961–1972, doi:10.1002/hyp.7328, 2009. 1053

Bavera, D., Bavay, M., Jonas, T., Lehning, M., and De Michele, C.: A comparison between two statistical and a physically-based model in snow water equivalent mapping, Adv. Water Resour., 63, 167–178, doi:10.1016/j.advwatres.2013.11.011, 2014. 1048, 1049, 1054

Blöschl, G. and Kirnbauer, R.: An analysis of snow cover patterns in a small alpine catchment, Hydrol. Process., 6, 99–109, doi:10.1002/hyp.3360060109, 1992. 1050
Carroll, S. S. and Cressie, N.: Spatial modeling of snow water equivalent using covariances estimated from spatial and geomorphic attributes, J. Hydrol., 190, 42–59, doi:10.1016/S0022-1694(96)03062-4, 1996. 1049, 1054
Church, J. E.: Snow surveying: its principles and possibilities, Geogr. Rev., 23, 529–563, 1933. 1053
Colomina, I. and Molina, P.: Unmanned aerial systems for photogrammetry and remote sensing: a review, ISPRS J. Photogramm., 92, 79–97, doi:10.1016/j.isprsjprs.2014.02.013, 2014. 1050, 1052
Cox, L., Bartee, L., Crook, A., Farnes, P., and Smith, J.: The care and feeding of snow pillows, in: Proceedings of the 46th Annual Western Snow Conference, Otter Rock, Oregon, 40–47, 1978. 1049, 1050
Dadic, R., Mott, R., Lehning, M., and Burlando, P.: Wind influence of snow depth distribution and accumulation over glaciers, J. Geophys. Res., 115, F01012, doi:10.1029/2009JF001261, 2010. 1050
Deems, J. S., Fassnacht, S. R., and Elder, K. J.: Fractal distribution of snow depth from lidar data, J. Hydrometeorol., 7, 285–297, doi:10.1175/JHM487.1, 2006. 1050
Deems, J. S., Painter, T. H., and Finnegan, D. C.: Lidar measurement of snow depth: a review, J. Glaciol., 59, 467–479, doi:10.3189/2013JoG12J154, 2013. 1050, 1051, 1053
Delacourt, C., Allemand, P., Jaud, M., Grandjean, P., Deschamps, A., Ammann, J., Cuq, V., and Suanez, S.: DRELIO: an unmanned helicopter for imaging coastal areas, J. Coastal Res., 56, 1489–1493, 2009. 1052
Dietz, A. J., Kuenzer, C., Gessner, U., and Dech, S.: Remote sensing of snow – a review of available methods, Int. J. Remote Sens., 33, 4094–4134, doi:10.1080/01431161.2011.640964, 2012. 1050
Dressler, K. A., Leavesley, G. H., Bales, R. C., and Fassnacht, S. R.: Evaluation of gridded snow water equivalent and satellite snow cover products for mountain basins in a hydrologic model, Hydrol. Process., 20, 673–688, doi:10.1002/hyp.6130, 2006. 1049, 1054
Dunford, R., Michel, K., Gagnage, M., Piegay, H., and Tremelo, M. L.: Potential and constraints of unmanned aerial vehicle technology for the characterization of Mediterranean riparian forest, Int. J. Remote Sens., 30, 4915–4935, 2009. 1052

Eisenbeiss, H.: UAV Photogrammetry, 194, Institute of Geodesy and Photogrammetry, ETH Zürich, 2009. 1052

Elder, K., Dozier, J., and Michaelsen, J.: Snow accumulation and distribution in an alpine watershed, Water Resour. Res., 27, 1541–1552, doi:10.1029/91WR00506, 1991. 1048, 1054

Elder, K., Rosenthal, W., and Davis, R. E.: Estimating the spatial distribution of snow water equivalence in a montane watershed, Hydrol. Process., 12, 1793–1808, 1998. 1049

Ellis, C. R., Pomeroy, J. W., Brown, T., and MacDonald, J.: Simulation of snow accumulation and melt in needleleaf forest environments, Hydrol. Earth Syst. Sci., 14, 925–940, doi:10.5194/hess-14-925-2010, 2010. 1049

Erxleben, J., Elder, K., and Davis, R.: Comparison of spatial interpolation methods for estimating snow distribution in the Colorado Rocky Mountains, Hydrol. Process., 16, 3627–3649, doi:10.1002/hyp.1239, 2002. 1049, 1054

Farinotti, D., Magnusson, J., Huss, M., and Bauder, A.: Snow accumulation distribution inferred from time-lapse photography and simple modelling, Hydrol. Process., 24, 2087–2097, doi:10.1002/hyp.7629, 2010. 1050

Fassnacht, S. R.: Estimating alter-shielded gauge snowfall undercatch, snowpack sublimation, and blowing snow transport at six sites in the coterminous USA, Hydrol. Process., 18, 3481–3492, 2004. 1050

Fassnacht, S. R., Dressler, K. A., and Bales, R. C.: Snow water equivalent interpolation for the Colorado River Basin from snow telemetry (SNOTEL) data, Water Resour. Res., 39, 1208, 2003. 1054, 1059

Funaki, M., Hirasawa, N., and the Ant Plane Group: Outline of a small unmanned aerial vehicle (Ant-Plane) designed for Antarctic research, Polar Science, 2, 129–142, 2008. 1052, 1060

Golding, D. L. and Swanson, R. H.: Snow distribution patterns in clearings and adjacent forest, Water Resour. Res., 22, 1931–1940, doi:10.1029/WR022i013p01931, 1986. 1049

Grünewald, T. and Lehning, M.: Are flat-field snow depth measurements representative? A comparison of selected index sites with areal snow depth measurements at the small catchment scale, Hydrol. Process., doi:10.1002/hyp.10295, in press, 2014. 1049, 1050, 1058, 1059

Grünewald, T., Schirmer, M., Mott, R., and Lehning, M.: Spatial and temporal variability of snow depth and ablation rates in a small mountain catchment, The Cryosphere, 4, 215–225, doi:10.5194/tc-4-215-2010, 2010. 1048, 1049, 1050

Grünewald, T., Stötter, J., Pomeroy, J. W., Dadic, R., Moreno Baños, I., Marturià, J., Spross, M., Hopkinson, C., Burlando, P., and Lehning, M.: Statistical modelling of the snow depth distribution in open alpine terrain, Hydrol. Earth Syst. Sci., 17, 3005–3021, doi:10.5194/hess-17-3005-2013, 2013. 1048, 1049, 1050

Gutmann, E. D., Larson, K. M., Williams, M. W., Nievinski, F. G., and Zavorotny, V.: Snow measurement by GPS interferometric reflectometry: an evaluation at Niwot Ridge, Colorado, Hydrol. Process., 26, 2951–2961, 2012. 1053

Harshburger, B. J., Humes, K. S., Walden, V. P., Blandford, T. R., Moore, B. C., and Dezzani, R. J.: Spatial interpolation of snow water equivalency using surface observations and remotely sensed images of snow-covered area, Hydrol. Process., 24, 1285–1295, doi:10.1002/hyp.7590, 2010. 1054

Hedrick, A., Marshall, H.-P., Winstral, A., Elder, K., Yueh, S., and Cline, D.: Independent evaluation of the SNODAS snow depth product using regional-scale lidar-derived measurements, The Cryosphere, 9, 13–23, doi:10.5194/tc-9-13-2015, 2015. 1050

Hinckley, E.-L. S., Ebel, B. A., Barnes, R. T., Anderson, R. S., Williams, M. W., and Anderson, S. P.: Aspect control of water movement on hillslopes near the rain – snow transition of the Colorado Front Range, Hydrol. Process., 28, 74–85, doi:10.1002/hyp.9549, 2014. 1049

Hirashima, H., Yamaguchi, S., and Katsushima, T.: A multi-dimensional water transport model to reproduce preferential flow in the snowpack, Cold Reg. Sci. Technol., 108, 80–90, 2014. 1048

Hock, R.: A distributed temperature-index ice- and snowmelt model including potential direct solar radiation, J. Glaciol., 45, 101–111, 1999. 1049

Hopkinson, C., Sitar, M., Chasmer, L., and Treitz, P.: Mapping snowpack depth beneath forest canopies using airborne lidar, Photogramm. Eng. Rem. S., 70, 323–330, 2004. 1050

Hopkinson, C., Collins, T., Anderson, A., Pomeroy, J., and Spooner, I.: Spatial snow depth assessment using LiDAR transect samples and public GIS data layers in the Elbow River Watershed, Alberta, Can. Water Resour. J., 37, 69–87, doi:10.4296/cwrj3702893, 2012. 1050

Hugenholtz, C. H., Whitehead, K., Brown, O. W., Barchyn, T. E., Moorman, B. J., LeClair, A., Riddell, K., and Hamilton, T.: Geomorphological mapping with a small unmanned aircraft system (sUAS): feature detection and accuracy assessment of a photogrammetrically-derived digital terrain model, Geomorphology, 194, 16–24, doi:10.1016/j.geomorph.2013.03.023, 2013. 1052

Johnson, J. B.: A theory of pressure sensor performance in snow, Hydrol. Process., 18, 53–64, doi:10.1002/hyp.1310, 2004. 1050
Katsushima, T., Yamaguchi, S., Kumakura, T., and Sato, A.: Experimental analysis of preferential flow in dry snowpack, Cold Reg. Sci. Technol., 85, 206–216, doi:10.1016/j.coldregions.2012.09.012, 2013. 1048
Klos, P. Z., Link, T. E., and Abatzoglou, J. T.: Extent of the rain-snow transition zone in the western U.S. under historic and projected climate, Geophys. Res. Lett., 41, 4560–4568, doi:10.1002/2014GL060500, 2014. 1049
Koh, L. P. and Wich, S. A.: Dawn of drone ecology: low-cost autonomous aerial vehicles for conservation, Trop. Conserv. Sci., 5, 121–132, 2012. 1052
König, M. and Sturm, M.: Mapping snow distribution in the Alaskan Arctic using aerial photography and topographic relationships, Water Resour. Res., 34, 3471–3483, doi:10.1029/98WR02514, 1998. 1050
Lehning, M. and Fierz, C.: Assessment of snow transport in avalanche terrain, Cold Reg. Sci. Technol., 51, 240–252, doi:10.1016/j.coldregions.2007.05.012, 2008. 1049
Lehning, M., Völksch, I., Gustafsson, D., Nguyen, T. A., Stähli, M., and Zappa, M.: ALPINE3D: a detailed model of mountain surface processes and its application to snow hydrology, Hydrol. Process., 20, 2111–2128, doi:10.1002/hyp.6204, 2006. 1049
Lehning, M., Löwe, H., Ryser, M., and Raderschall, N.: Inhomogeneous precipitation distribution and snow transport in steep terrain, Water Resour. Res., 44, W07404, doi:10.1029/2007WR006545, 2008. 1049
Lehning, M., Grünewald, T., and Schirmer, M.: Mountain snow distribution governed by an altitudinal gradient and terrain roughness, Geophys. Res. Lett., 38, L19504, doi:10.1029/2011GL048927, 2011. 1050
Lejot, J., Delacourt, C., Piégay, H., Fournier, T., Trémélo, M. L., and Allemand, P.: Very high spatial resolution imagery for channel bathymetry and topography from an unmanned mapping controlled platform, Earth Surf. Proc. Land., 32, 1705–1725, 2007. 1052
López Moreno, J. I. and Nogués-Bravo, D.: Interpolating local snow depth data: an evaluation of methods, Hydrol. Process., 20, 2217–2232, doi:10.1002/hyp.6199, 2006. 1049, 1054
Lundquist, J. D. and Dettinger, M. D.: How snowpack heterogeneity affects diurnal streamflow timing, Water Resour. Res., 41, W05007, doi:10.1029/2004WR003649, 2005. 1048
Luzi, G., Noferini, L., Mecatti, D., Macaluso, G., Pieraccini, M., Atzeni, C., Schaffhauser, A., Fromm, R., and Nagler, T.: Using a ground-based SAR interferometer and a terrestrial laser

scanner to monitor a snow-covered slope: results from an experimental data collection in Tyrol (Austria), IEEE T. Geosci. Remote, 47, 382–393, doi:10.1109/TGRS.2008.2009994, 2009. 1050

Machguth, H., Eisen, O., Paul, F., and Hoezle, M.: Strong spatial variability of snow accumulation observed with helicopter-borne GPR on two adjacent Alpine glaciers, Geophys. Res. Lett., 33, L13503, doi:10.1029/2006GL026576, 2006. 1053

Marks, D., Winstral, A., Reba, M., Pomeroy, J., and Kumar, M.: An evaluation of methods for determining during-storm precipitation phase and the rain/snow transition elevation at the surface in a mountain basin, Adv. Water Resour., 55, 98–110, doi:10.1016/j.advwatres.2012.11.012, 2013. 1049

Marsh, C. B., Pomeroy, J. W., and Spiteri, R. J.: Implications of mountain shading on calculating energy for snowmelt using unstructured triangular meshes, Hydrol. Process., 26, 1767–1778, doi:10.1002/hyp.9329, 2012. 1049

Molotch, N. P., Fassnacht, S. R., Bales, R. C., and Helfrich, S. R.: Estimating the distribution of snow water equivalent and snow extent beneath cloud cover in the Salt–Verde River basin, Arizona, Hydrol. Process., 18, 1595–1611, doi:10.1002/hyp.1408, 2004. 1049

Morin, S., Lejeune, Y., Lesaffre, B., Panel, J.-M., Poncet, D., David, P., and Sudul, M.: An 18-yr long (1993–2011) snow and meteorological dataset from a mid-altitude mountain site (Col de Porte, France, 1325 m alt.) for driving and evaluating snowpack models, Earth Syst. Sci. Data, 4, 13–21, doi:10.5194/essd-4-13-2012, 2012. 1049

Mott, R. and Lehning, M.: Meteorological modeling of very high-resolution wind fields and snow deposition for mountains, J. Hydrometeorol., 11, 934–949, doi:10.1175/2010JHM1216.1, 2010. 1049

Mott, R., Egli, L., Grünewald, T., Dawes, N., Manes, C., Bavay, M., and Lehning, M.: Micrometeorological processes driving snow ablation in an Alpine catchment, The Cryosphere, 5, 1083–1098, doi:10.5194/tc-5-1083-2011, 2011. 1048

Mott, R., Scipión, D., Schneebeli, M., Dawes, N., and Lehning, M.: Orographic effects on snow deposition patterns in mountainous terrain, J. Geophys. Res., 119, 1419–1439, doi:10.1002/2013JD019880, 2014. 1049

Nievinski, F. G. and Larson, K. M.: Inverse modeling of GPS multipath for snow depth estimation – Part II: Application and validation, IEEE T. Geosci. Remote, 52, 6555–6563, 2014. 1053

Parajka, J. and Blöschl, G.: Validation of MODIS snow cover images over Austria, Hydrol. Earth Syst. Sci., 10, 679–689, doi:10.5194/hess-10-679-2006, 2006. 1050

Pollefeys, M., Koch, R., and Van Gool, L.: Self-calibration and metric reconstruction in spite of varying and unknown internal camera parameters, in: IJCV, Sixth International Conference on Computer Vision, Bombay, India, 90–95, doi:10.1109/ICCV.1998.710705, 1999. 1052
Pomeroy, J., Fang, X., and Ellis, C.: Sensitivity of snowmelt hydrology in Marmot Creek, Alberta, to forest cover disturbance, Hydrol. Process., 26, 1891–1904, doi:10.1002/hyp.9248, 2012. 1049
Prokop, A., Schirmer., M., Rub, M., Lehning, M., and Stocker, M.: A comparison of measurement methods: terrestrial laser scanning, tachymetry and snow probing for the determination of the spatial snow-depth distribution on slopes, Ann. Glaciol., 49, 210–216, doi:10.3189/172756408787814726, 2008. 1050, 1053
Remondino, F.: Detectors and descriptors for photogrammetric applications, ISPRS Archives, 36, 49–54, 2006. 1052
Remondino, F. and El-Hakim, S.: Image-based 3D modelling: a review, Photogram. Record, 21, 269–291, 2006. 1056
Ryan, W. A., Doesken, N. J., and Fassnacht, S. R.: Evaluation of ultrasonic snow depth sensors for U.S. snow measurements, J. Atmos. Ocean. Tech., 25, 667–684, doi:10.1175/2007JTECHA947.1, 2008. 1049
Schweizer, J., Kronholm, K., Bruce Jamieson, J., and Birkeland, K. W.: Review of spatial variability of snowpack properties and its importance for avalanche formation, Cold Reg. Sci. Technol., 51, 253–272, doi:10.1016/j.coldregions.2007.04.009, 2008. 1048
Scipión, D., Mott, R., Lehning, M., Schneebeli, M., and Berne, A.: Seasonal small-scale spatial variability in alpine snowfall and snow accumulation, Water Resour. Res., 49, 1446–1457, doi:10.1002/wrcr.20135, 2013. 1048
Skaugen, T.: Modelling the spatial variability of snow water equivalent at the catchment scale, Hydrol. Earth Syst. Sci., 11, 1543–1550, doi:10.5194/hess-11-1543-2007, 2007. 1049
Sona, G., Pinto, L., Pagliari, D., Passoni, D., and Gini, R.: Sperimental analysis of different software packages for orientation and digital surface modelling from UAV images, Earth Sci. Inform., 7, 97–107, doi:10.1007/s12145-013-0142-2, 2014. 1052
Stretcha, C., Pylyänäinen, T., and Fua, P.: Dynamic and scalable large scale image reconstruction, in: IEEE Conference on Computer Vision and Pattern Recognition, San Francisco, USA, 406–413, doi:10.1109/CVPR.2010.5540184, 2010. 1052

Watts, A. C., Ambrosia, V. G., and Hinkley, E. A.: Unmanned aircraft systems in remote sensing and scientific research: classification and considerations of use, Remote Sensing, 4, 1671–1692, doi:10.3390/rs4061671, 2012. 1050, 1052

Winstral, A., Marks, D., and Gurney, R.: Simulating wind-affected snow accumulations at catchment to basin scales, Adv. Water Resour., 55, 64–79, doi:10.1016/j.advwatres.2012.08.011, 2013. 1048

Worby, A. P., Markus, T., Steer, A. D., Lytle, V. I., and Massom, R. A.: Evaluation of AMSR-E snow depth product over East Antarctic sea ice using in situ measurements and aerial photography, J. Geophys. Res., 113, C05S94, doi:10.1029/2007JC004181, 2008. 1050

Table 1. Comparison between manual (H_M) and U.A.S. ($H_{U.A.S.}$) snow depth measurements.

ID	H_M [m]	$H_{U.A.S.}$ [m]	$H_M - H_{U.A.S.}$ [m]
1	1.48	1.40	0.08
2	2.07	2.06	0.01
3	1.75	1.96	−0.21
4	1.88	2.05	−0.17
5	1.68	1.93	−0.25
6	1.85	2.13	−0.28
7	1.96	2.03	−0.07
8	2.11	2.17	−0.06
9	1.91	1.96	−0.05
10	1.89	1.81	0.08
11	1.45	1.49	−0.04
12	1.60	1.52	0.08
Average difference [m]			−0.073
SD difference [m]			0.128

TCD
9, 1047–1075, 2015

Snow depth variability using U.A.S.

C. De Michele et al.

Table 2. Snow volume calculation using U.A.S. measurements and three different spatial resolutions: 5, 10, 20 cm.

Resolution [cm]	pixels [#]	$\bar{H}$ [m]	H_{max} [m]	H_{min} [m]	V [m^3]
5	81 918 743	2.26	4.21	−0.22	463 652.3
10	20 479 686	2.26	4.35	−0.24	462 957.8
20	5 119 921	2.27	4.15	−0.24	464 093.0

TCD
9, 1047–1075, 2015

Table 3. Comparison between the snow volume via U.A.S. $V_{\text{U.A.S.}} = 463\,652.3\,\text{m}^{-3}$ and the one obtained via spatialization techniques (V_T).

Technique	V_T [m^3]	$V_{\text{U.A.S.}} - V_\text{T}$ [m^3]
Arith.c mean	369 146.3	94 505.9
IDW	368 216.9	95 435.3
Thiessen	363 400.5	100 251.7
Kriging	368 433.1	95 219.2

TCD
9, 1047–1075, 2015
Snow depth variability using U.A.S.
C. De Michele et al.

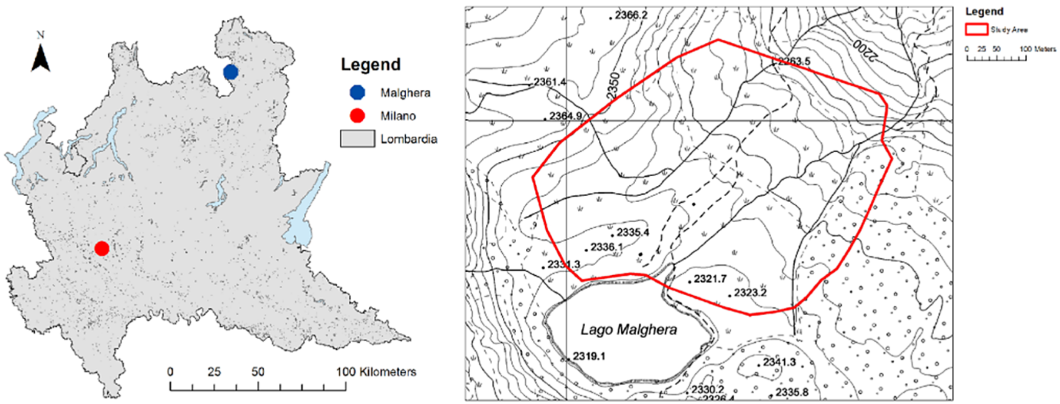

Figure 1. Location of the study area in western Val Grosina valley, Lombardy region, northern Italy. In the right panel, it is reported the topographic map of the area in scale 1 : 10 000, with isolines every 10 m and the elevation (in m) of some points of interest.

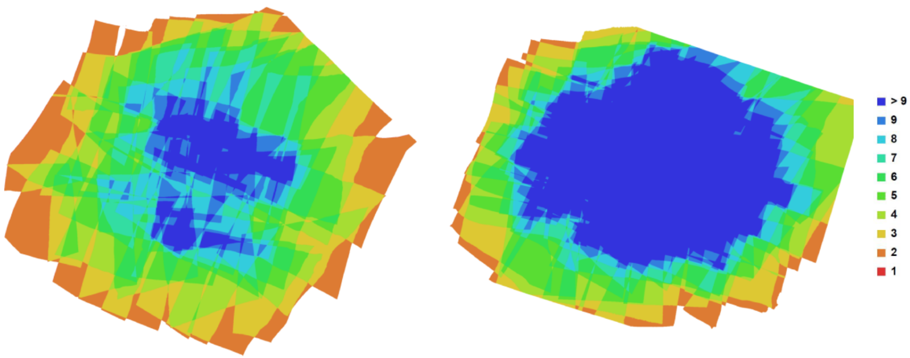

Figure 2. Camera images and their overlaps during each of the two surveys. The left panel refers to the survey made during September 2013, while the right panel regards the survey made in April 2014. The legend indicates the number of images covering each area.

TCD
9, 1047–1075, 2015

Snow depth variability using U.A.S.

C. De Michele et al.

Title Page
Abstract Introduction
Conclusions References
Tables Figures
◀◀ ▶▶
◀ ▶
Back Close
Full Screen / Esc
Printer-friendly Version
Interactive Discussion

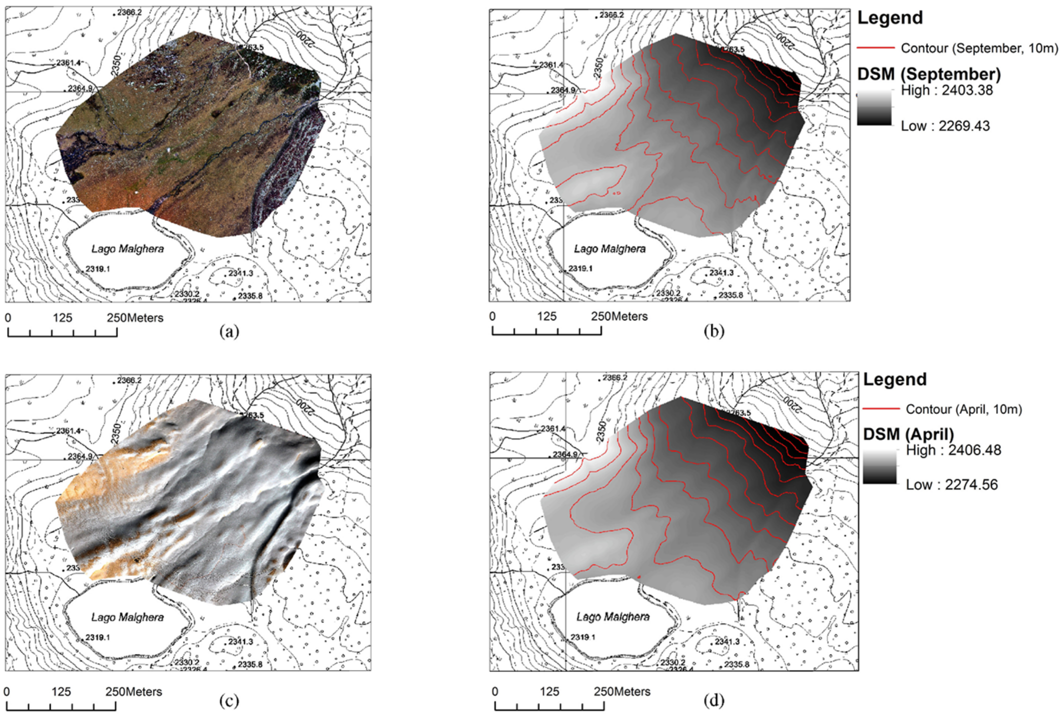

Figure 3. Ortophotos and Digital Surface Models (DSM) of the two surveys. **(a)** reports the ortophoto of the survey run in September 2013, while **(b)** depicts the associated DSM. Similarly, **(c, d)** report the ortophoto and the DSM of the April 2014 survey, respectively.

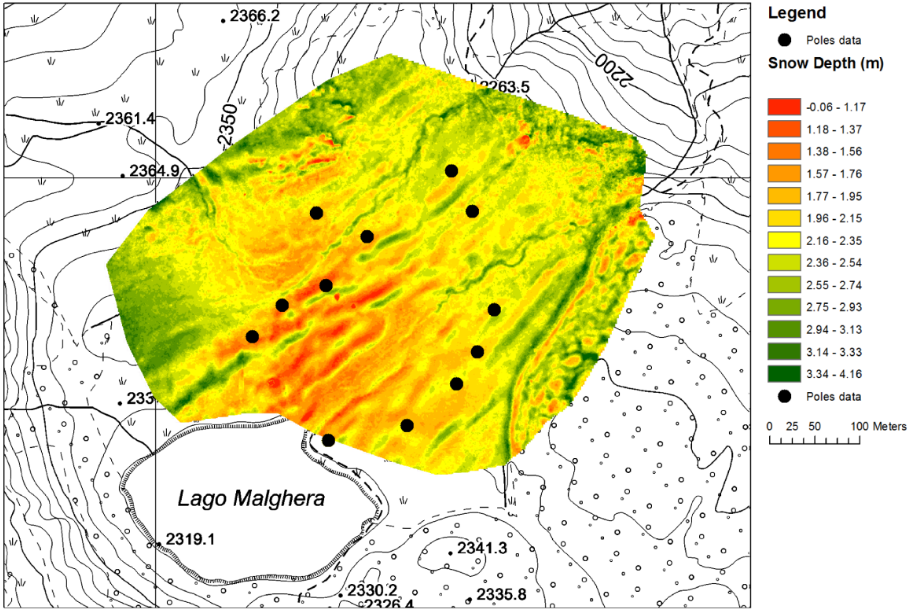

Figure 4. A map of snow depth distribution over the study area, obtained by means of difference of the elevations of the maps reported in Fig. 3. Different colors indicate different values of snow thicnkess (see the legend scale). Black dots indicate the location of the 12 manual measurements of snow depth.

TCD
9, 1047–1075, 2015